

Decision-Tree Models Indicative of Microvascular Invasion on MRI Predict Survival in Patients with Hepatocellular Carcinoma Following Tumor Ablation

Robin Schmidt^{1,2}, Charlie Alexander Hamm^{1,3}, Christopher Rueger¹, Han Xu¹, Yubei He^{1,2}, Luzie Alexandra Gottwald⁴, Bernhard Gebauer¹, Lynn Jeanette Savic¹⁻³

¹Charité – Universitätsmedizin Berlin, Corporate Member of Freie Universität Berlin and Humboldt-Universität zu Berlin, Department of Radiology, Berlin, 13353, Germany; ²Experimental Clinical Research Center (ECRC) at Charité - Universitätsmedizin Berlin and Max-Delbrück-Centrum für Molekulare Medizin (MDC), Berlin, 13125, Germany; ³Berlin Institute of Health at Charité – Universitätsmedizin Berlin, Berlin, 10117, Germany; ⁴Vivantes Humboldt-Klinikum, Berlin, 13509, Germany

Correspondence: Lynn Jeanette Savic, Charité Universitätsmedizin Berlin, Campus Virchow Klinikum, Klinik für Radiologie, Augustenburger Platz 1, Berlin, D-13353, Germany, Email lynn-jeanette.savic@charite.de

Purpose: Histological microvascular invasion (MVI) is a risk factor for poor survival and early recurrence in hepatocellular carcinoma (HCC) after surgery. Its prognostic value in the setting of locoregional therapies (LRT), where no tissue samples are obtained, remains unknown. This study aims to establish CT-derived indices indicative of MVI on liver MRI with superior soft tissue contrast and evaluate their association with patient survival after ablation via interstitial brachytherapy (iBT) versus iBT combined with prior conventional transarterial chemoembolization (cTACE).

Patients and Methods: Ninety-five consecutive patients, who underwent ablation via iBT alone (n = 47) or combined with cTACE (n = 48), were retrospectively included between 01/2016 and 12/2017. All patients received contrast-enhanced MRI prior to LRT. Overall (OS), progression-free survival (PFS), and time-to-progression (TTP) were assessed. Decision-tree models to determine Radiogenomic Venous Invasion (RVI) and Two-Trait Predictor of Venous Invasion (TTPVI) on baseline MRI were established, validated on an external test set (TCGA-LIHC), and applied in the study cohorts to investigate their prognostic value for patient survival. Statistics included Fisher's exact and *t*-test, Kaplan–Meier and cox-regression analysis, area under the receiver operating characteristic curve (AUC-ROC) and Pearson's correlation.

Results: OS, PFS, and TTP were similar in both treatment groups. In the external dataset, RVI showed low sensitivity but relatively high specificity (AUC-ROC = 0.53), and TTPVI high sensitivity but only low specificity (AUC-ROC = 0.61) for histological MVI. In patients following iBT alone, positive RVI and TTPVI traits were associated with poorer OS (RVI: $p < 0.01$; TTPVI: $p = 0.08$), PFS ($p = 0.04$; $p = 0.04$), and TTP ($p = 0.14$; $p = 0.03$), respectively. However, when patients with combined cTACE and iBT were stratified by RVI or TTPVI, no differences in OS ($p = 0.75$; $p = 0.55$), PFS ($p = 0.70$; $p = 0.43$), or TTP ($p = 0.33$; $p = 0.27$) were observed.

Conclusion: The study underscores the role of non-invasive imaging biomarkers indicative of MVI to identify patients, who would potentially benefit from embolotherapy via cTACE prior to ablation rather than ablation alone.

Keywords: cancer imaging, hepatocellular carcinoma, microvascular invasion, magnetic resonance tomography, predictive imaging biomarkers

Introduction

Hepatocellular carcinoma (HCC) is the most common primary liver malignancy and the third leading cause of cancer-related death worldwide.¹ In unresectable, loco-regional therapies (LRT) are guideline-approved first-line therapies including ablation therapies for early disease stages and conventional transarterial chemoembolization (cTACE) for intermediate stage disease, respectively.^{2,3} In comparison to thermal ablation techniques such as radiofrequency (RF) or microwave ablation (MWA), non-thermal ablation using CT-guided interstitial high-dose rate brachytherapy (iBT) demonstrates promising median overall survival (OS) and time-to-progression (TTP) in patients with large (>5 cm)

and multifocal unresectable HCC.⁴ iBT comprises the catheter-based internal radiation of the tumor with a beta-emitting iridium-192 source being temporarily applied and removed immediately after treatment.^{5–7} Additionally, ablation can be combined with cTACE for the treatment of larger, earlier-stage HCCs up to 5 cm, where ablation alone is insufficient for complete treatment leading to high rates of local recurrence.⁸ Given the hypervascularized nature of HCC, a combination of iBT with cTACE tries to exploit the additive benefits of local radiation and embolization with promising efficacy.⁴ Besides radiographical tumor size and hypervascularization, the tumor's histological phenotype may also affect susceptibility to LRT.⁹ Specifically, microvascular invasion (MVI) represents tumor angiogenesis and a more aggressive tumoral phenotype that impacts both disease-free and OS in patients with HCC.¹⁰ So far, MWI may only be assessed post-operatively by histopathological diagnosis and thus, it has only been validated as a predictor of early recurrence and poor survival after surgical regimens.¹¹ However, novel imaging biomarkers aim to link the vascular-specific HCC gene profile with semantic radiological imaging features to enable the non-invasive prediction of MVI. As single imaging features cannot fully capture MWI on cross-sectional imaging, novel diagnostic tools entail decision tree-like algorithms to enable the non-invasive diagnosis of MWI in HCC. Following the decoding of gene expression programs in liver cancer, single ancillary imaging findings in biomedical imaging have been linked with genomic profiles of pathologic liver tissue. Specifically, “Radiogenomic Venous Invasion” (RVI) and “Two-Trait Predictor of Venous Invasion” (TTPVI) represent two well-studied algorithms that include a decision-tree-like approach of a few of those imaging features to ensure higher reliability while being designed and validated on contrast-enhanced computed tomography (CECT) imaging.^{12,13} Clinical studies reported their potential to predict poorer clinical outcomes in patients undergoing surgical resection and orthotopic liver transplant (OLT)^{14–16} with good intra- and inter-observer agreement.¹⁷ However, their clinical prognostic value for HCC patients undergoing LRT has not yet been investigated. Moreover, the superior soft tissue contrast of contrast-enhanced magnetic resonance imaging (MRI) frequently outperforms CECT in the diagnosis and staging of HCC¹⁸ and is therefore more commonly found in the clinical routine for both diagnosis and follow-up. Therefore, the purpose of this study was to establish the CT-based decision-tree models for RVI and TTPVI as imaging biomarkers on liver MRI and to evaluate their potential association with OS, progression-free survival (PFS), and TTP in patients with HCC undergoing loco-regional therapies by means of iBT alone or combined with cTACE.

Materials and Methods

Study Cohort and Design

This retrospective single-center study was approved by the local institutional review board of the Charité – University Medicine Berlin. Informed consent was waived due to the retrospective study design. The study protocol covers patient data confidentially and conforms with the ethical guidelines of the Declaration of Helsinki as reflected in a prior approval by the Charité – University Medicine Berlin's human research committee. Consecutive patients with the primary diagnosis of unresectable HCC following LRT between 01/2016 and 12/2017 were included in two groups: one group with patients undergoing iBT alone and the other group with patients following a prior cTACE before iBT. The primary HCC diagnosis was confirmed via imaging or histopathology. All target lesions were naïve to minimally invasive liver-directed therapies. Additional eligibility criteria included contrast-enhanced MRI within 30 days prior to LRT, availability of patient demographics and survival data, and regular follow-up imaging eight weeks after LRT, then every three months for the first year and every six months for the following years, over a minimum of 12 months and a maximum of a 4-year follow-up period to ensure an adequate follow-up time frame for survival analysis.

Additionally, a public external dataset (The Cancer Genome Atlas – Liver Hepatocellular Carcinoma, TCGA-LIHC) was used to validate CT-based indices RVI and TTPVI on liver MRI. The database includes patients with primary liver cancer following surgical resection providing pre-procedural imaging and post-procedural histological confirmation of MVI. Thirty-eight of these patients had a confirmed HCC diagnosis, contrast-enhanced MR imaging, and histological reports.¹⁹

The primary endpoint was to establish the assessment of RVI and TTPVI for the prediction of MVI on pre-procedural MRI (external group), following the evaluation of their predictive value for OS, PFS, and TTP in terms of ablation via iBT alone or in combination with an embolization via a prior cTACE before iBT (internal study groups). Secondary endpoints

included correlations of the imaging biomarkers with local tumor progression (LTP) and intrahepatic distant recurrence (IDR) subtypes of PFS and TTP, as well as the correlation of RVI and TTPVI with other semantic imaging features.

Locoregional therapies. The decision for LRT was reached in consensus by the institutional multidisciplinary tumor board. Recommendations for iBT alone or in combination with cTACE were given at the discretion of the interventional radiologist. LRT procedures follow the guideline recommendations described elsewhere^{20–22} and are explicitly described in the [Supplement Material](#).

Image Acquisition and Analysis

Image analysis was performed by two radiologists with three and eight years of experience in abdominal imaging, who did not allocate or perform the LRT. The MRI protocol is described in the [Supplement Material](#). Briefly, the standard protocol included multiparametric imaging including breath-hold unenhanced and contrast-enhanced T1-weighted imaging using a hepatocyte-specific contrast agent (Primovist, Bayer, Germany).

RVI and TTPVI Algorithm Establishment and Semantic Imaging Features

Both RVI and TTPVI decision tree algorithms were adapted from previous studies based on CECT and established on MRI.^{13–16} RVI trait's algorithm included the persistent enhancement of intratumoral vessels in the portal venous phase of T1-weighted images, followed by the absence of a hypointense halo partially or completely circumscribing the tumor in the portal venous phase, and the absence of a sharp transition between tumor and adjacent liver parenchyma in the portal venous phase. In comparison, TTPVI trait's algorithm contained the presence of intratumoral vessels in the arterial phase in the absence of a hypointense halo in the portal venous phase of T1-weighted images, while the tumor-liver difference was no semantic feature within the algorithm ([Figure 1](#)). In patients with multiple lesions, the largest tumor was considered as the index lesion. RVI and TTPVI were correlated with other semantic imaging features within the internal study cohorts and with histopathological MVI within the TCHA-LIHC cohort. Semantic imaging features and their

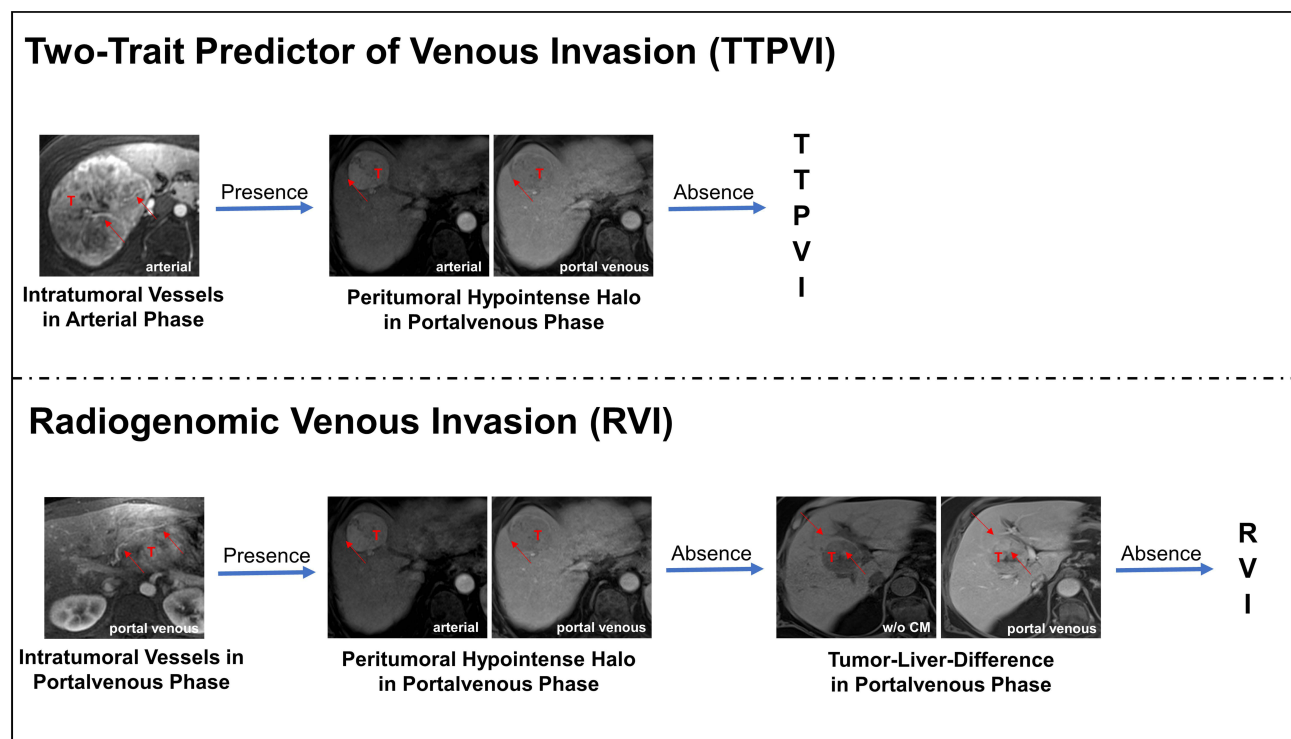


Figure 1 TTPVI and RVI are defined by a two- and three-trait tree-like decision model, respectively. TTPVI (upper row):¹³ Index lesion must include the presence of intratumoral vessels in arterial contrast phase followed by the absence of a peritumoral hypointense halo in the portal venous contrast phase. RVI (lower row):¹⁴ Index lesion must include the presence of intratumoral vessels in portal venous contrast phase, followed by the absence of a peritumoral hypointense halo in the portal venous contrast phase, and moreover, followed by the absence of a sharp tumor-liver-difference in the portal venous contrast phase. Arrows indicate the respective imaging trait. T indicated the tumoral index lesion.

assessment are listed in the [Supplement Material](#) and briefly include imaging features of the tumor or the peripheral zone in dynamic contrast-enhanced and hepatobiliary phase of T1-weighted images, diffusion-weighted imaging (DWI), and apparent diffusion coefficient (ADC) maps.

Tumor Response Assessment

Tumor response was assessed according to modified response evaluation criteria in solid tumors (mRECIST)²³ on follow-up MRI scans by two radiologists with three and eight years of experience in abdominal imaging, respectively.

Survival Analysis and Patterns of Progression

Survival analyses were performed for all internal and the external cohorts. Medical records were reviewed using the institution's oncologic database. The last follow-up data collection was performed on July 15th, 2021. OS, PFS, and TTP (definitions in [Supplement Material](#)) were analyzed using Kaplan–Meier analysis and Log rank testing as defined elsewhere.²⁴ In addition, univariate cox-regression analysis was performed to evaluate the predictive value of RVI and TTPVI on survival outcomes, and to estimate for the confounding effect of the cohorts' baseline characteristics. Relevant parameters from the univariate model (p -value <0.1) were incorporated into a multivariate Cox regression model.

Local and Distant Intrahepatic Tumor Recurrence

Besides OS, PFS, and TTP, two specific progression patterns were assessed for subgroup analyses considering intrahepatic local tumor progression (LTP, PFS_{LTP} and TTP_{LTP}) and intrahepatic distant tumor recurrence (IDR, PFS_{IDR} and TTP_{IDR}). LTP describes the reappearance of the target lesion within or adjacent to the ablation zone, while IDR considered the occurrence of new intrahepatic lesions that were not spatially associated with the primary target lesion.^{25,26}

Statistics

Descriptive statistics were reported as numbers and percentages or mean and standard deviation. Statistics included Fisher's exact test for comparing categorical parameters, normality testing, t-testing, and Mann–Whitney-U testing for comparing metric parameters for the patient and tumor characteristics, Kaplan–Meier analysis with hazard ratio (HR) and 95%-confidence interval (95%-CI) calculation for comparing survival outcomes with the imaging biomarkers of RVI and TTPVI, and MVI in the external study cohort, qualitative performance metrics including sensitivity, specificity, positive and negative predictive values, area under the receiver operating characteristic curve (AUC-ROC), and last, Pearson correlation testing for comparing RVI and TTPVI traits with semantic imaging features. Statistical significance was defined as a p -value <0.05 . Statistics were performed using GraphPad Prism v9.0.0 (GraphPad, La Jolla, USA).

Results

Patient Characteristics in the Study Cohort

In total, 47 patients with 89 target tumors following iBT and 48 patients with 70 target tumors following cTACE/iBT were included. Thirteen patients received multiple completed treatments being separately considered for the calculation of TTP. Patient demographics and tumor characteristics are summarized in [Table 1](#). Briefly, the mean age was 70.6 ± 9.3 and 70.3 ± 9.5 years in patients treated with iBT and cTACE/iBT and 79.2% and 76.6% were men, respectively. Overall, baseline characteristics were comparable in both treatment groups except for index lesion diameter ($p < 0.01$) and BCLC stage ($p < 0.01$). Their confounding effects on patients' survival were accounted for in the Cox regression model.

RVI/TTPVI Establishment on Liver MRI and Cross-Validation in External TCGA Cohort

Assessment of both RVI and TTPVI in MRI was feasible. A positive TTPVI trait was more frequently observed in patients receiving cTACE/iBT as compared to iBT alone ($n = 28$, 60.9% vs $n = 19$, 40.4%, $p = 0.06$), while the presence of a positive RVI trait was similar in both groups ($n = 15$, 32.6% vs $n = 14$, 29.8%, $p = 0.82$). Due to the poor image quality of the external validation cohort, imaging biomarker assessment was feasible for 32 cases, in which TTPVI appeared in $n = 20$ (62.5%), RVI in $n = 11$ (34.4%) of patients, while histological MVI was confirmed in $n = 13$ (40.5%)

Table 1 Patients, Tumor and Disease Characteristics

Demographics	iBT Cohort	cTACE/iBT Cohort	p-value
Patient characteristics			
Number of patients	48	47	-
Number of completed therapies	60	51	0.68
Age, mean \pm SD	70.60 \pm 9.28 years	70.29 \pm 9.53 years	0.84
Male:Female, % (n)	79.2%:20.8% (38:10)	76.6%:23.4% (36:11)	0.81
Target tumor characteristics			
Lesions, n	89	70	-
Unifocal:Multifocal, % (n)	68.3%:31.7% (41:19)	74.5%:25.5% (38:13)	0.53
Index lesion diameter, mean \pm SD	26.51 \pm 10.58 mm	44.32 \pm 20.36 mm	<0.01
Disease characteristics			
Cirrhosis, % (n)	85.4% (41)	91.5% (43)	0.52
Etiology of cirrhosis, n (%)			
Hepatitis B	2.5% (1)	2.3% (2)	0.99
Hepatitis C	26.8% (11)	20.9% (9)	0.61
Alcoholic steatohepatitis	26.8% (11)	41.9% (18)	0.17
Non-alcoholic steatohepatitis	31.7% (13)	32.6% (14)	0.99
Others	12.2% (5)	-	-
Child Pugh class, % (n)			
A	82.9% (34)	97.7% (41)	0.09
B	17.1% (7)	2.3% (2)	0.09
Barcelona Clinic Liver Cancer stage, % (n)			
A	85.4% (41)	46.8% (22)	<0.01
B	12.5% (6)	36.2% (17)	0.01
C	2.1% (1)	17.0% (8)	0.02
Laboratory values of liver function, mean \pm SD			
Albumin [g/l]	38.7 \pm 6.6	38.7 \pm 3.7	0.96
Bilirubin [mg/dl]	0.76 \pm 0.53	0.82 \pm 0.47	0.23
ALT [U/l]	38.4 \pm 21.6	40.7 \pm 23.6	0.63
AST [U/l]	45.9 \pm 19.1	53.4 \pm 36.3	0.27
γ -GT [U/l]	162.7 \pm 154.0	195.0 \pm 179.0	0.24
AP [U/l]	115.0 \pm 60.8	106.1 \pm 46.6	0.73

Note: Bold p-values indicate statistical significance in the respective statistical test (Fisher's exact test, unpaired t-test, and Mann-Whitney U-test).

Abbreviations: iBT, interstitial brachytherapy; cTACE, conventional transarterial chemoembolization; ALT, alanine aminotransferase; AST, aspartate aminotransferase; γ -GT, gamma-glutamyl transferase; AP, alkaline phosphatase.

of the patients. RVI only showed low sensitivity (69.2%) but relatively high specificity (88.9%) and good positive (81.2%) and negative predictive values (80.0%) for MVI in the external dataset (AUC-ROC = 0.53). TTPVI showed a relatively high sensitivity (84.6%) and negative predictive value (81.2%) but only low specificity (50.0%) and positive predictive value (55.0%), respectively (AUC-ROC = 0.61).

Survival Outcomes and Analysis

Tumor Response

Tumor response at first and second follow-up is reported in Table 2. Briefly, the overall response rates were 84.4% at first and 64.6% at second follow-up for patients treated with iBT, as well as 61.7% at first and 66.7% at second follow-up for patients treated with cTACE/iBT, respectively.

Survival Analysis

During the follow-up period, 36 (76.6%) patients treated with iBT and 37 (77.1%) with cTACE/iBT had died, five patients (iBT: 4 vs cTACE/iBT: 1) underwent OLT, and 13 patients (9 vs 4) received an additional LRT on the target lesion. Median OS (iBT vs cTACE/iBT, 26.7 vs 23.7 months, $p = 0.49$), PFS (9.3 vs 7.7 months, $p = 0.36$) and TTP (9.8 vs 9.3 months, $p = 0.16$) did not differ between both treatment groups (Figure 2).

Association of RVI/TTPVI with Overall Survival

In patients with positive RVI and TTPVI traits, Kaplan–Meier analyses revealed poorer median OS for patients treated with iBT (positive vs negative, RVI 12.4 vs 40.4 months, $p < 0.01$, TTPVI 16.0 vs 37.7 months, $p = 0.08$). However, in patients treated with cTACE/iBT, stratification according to RVI or TTPVI status revealed no association with OS (RVI 26.0 vs 21.8 months, $p = 0.75$, TTPVI 25.6 vs 19.7 months, $p = 0.55$).

Association of RVI/TTPVI with Progression-Free Survival

In patients with positive RVI and TTPVI traits, Kaplan–Meier analyses revealed poorer median PFS for patients treated with iBT (RVI 5.9 vs 13.2 months, $p = 0.03$, TTPVI 5.9 vs 13.8 months, $p = 0.04$). However, in patients treated with cTACE/iBT, positive RVI or TTPVI traits revealed no significant impact for PFS (RVI 11.5 vs 6.2 months, $p = 0.70$, TTPVI 9.6 vs 6.5 months, $p = 0.43$). Moreover, in patients treated with iBT, positive traits were associated with poorer PFS_{LTP} (RVI $p < 0.01$, TTPVI $p = 0.02$) and PFS_{IDR} subtypes, respectively (RVI $p = 0.01$, TTPVI $p < 0.01$). Such findings could not be observed in patients treated with cTACE/iBT (Table 3).

Association of RVI/TTPVI with Time-to-Progression

In patients with positive RVI and TTPVI traits, Kaplan–Meier analyses revealed an association with poorer median TTP for patients treated with iBT (RVI 6.4 vs 11.8 months, $p = 0.14$, TTPVI 2.6 vs 5.9 months, $p = 0.03$), but not for patients treated with cTACE/iBT (RVI 14.2 vs 7.7 months, $p = 0.33$, TTPVI 12.1 vs 7.7 months, $p = 0.27$, Figure 3). For patients treated with iBT, positive traits were associated with poorer TTP_{IDR} subtype (RVI $p = 0.16$, TTPVI $p = 0.05$), but not in patients treated with cTACE/iBT (Table 3).

Table 2 Response Assessment Evaluation by Modified Response Criteria in Solid Tumors

mRECIST	8 Weeks		5 Months	
	iBT (n = 51)	cTACE/iBT (n = 47)	iBT (n = 48)	cTACE/iBT (n = 42)
CR	60.8% (31)	44.7% (21)	54.2% (26)	57.2% (24)
PR	23.6% (12)	17.0% (8)	10.4% (5)	9.5% (4)
SD	7.8% (4)	10.6% (5)	6.2% (3)	11.9% (5)
PD	7.8% (4)	27.7% (13)	29.2% (14)	21.4% (9)

Abbreviations: CR, complete response; PR, partial response; SD, stable disease; PD, progressive disease; iBT, interstitial brachytherapy; cTACE, conventional transarterial chemoembolization.

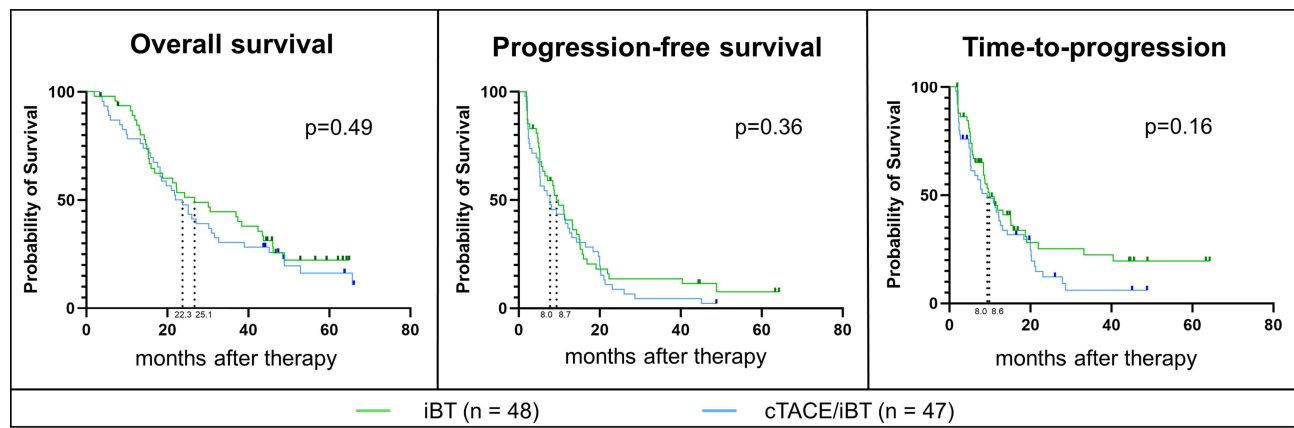


Figure 2 Patient survival and tumor progression with patients treated with ablation with and without prior embolization. Overall survival (OS), progression-free survival (PFS) and time-to-progression (TTP) are depicted for patients undergoing interstitial brachytherapy (iBT, green line) and conventional transarterial chemoembolization (cTACE, blue line). Kaplan–Meier analysis reveals no significant differences in survival outcomes between both patient groups. Median survival is indicated by dashed lines.

Association of RVI/TTPVI with Survival in the External TCGA Cohort

Patients in the external surgical TCGA-LIHC cohort had longer median OS (152.9 months, $p < 0.01$) and PFS (14.8 months, $p < 0.01$) as compared to the internal study cohorts. Patients with the presence of histological MVI showed no significant association but tended to have poorer OS (125.8 vs 170.8 months, $p = 0.35$) and PFS (12.6 vs 21.5 months,

Table 3 The Impact of Radiogenomic Venous Invasion (RVI) and Two-Trait Predictor of Venous Invasion (TTPVI) on Survival Outcomes

Outcome	Imaging Biomarker	iBT Cohort			cTACE/iBT Cohort		
		Positive	Negative	p-value	Positive	Negative	p-value
OS	TTPVI	15.97	37.65	0.08	25.58	19.72	0.55
	RVI	12.40	40.37	<0.01	26.03	21.77	0.75
PFS	TTPVI	5.87	13.77	0.04	9.58	6.45	0.43
	RVI	5.87	13.17	0.04	11.50	6.23	0.70
PFS _{LTP}	TTPVI	10.87	18.30	0.03	22.85	18.18	0.38
	RVI	8.73	17.73	<0.01	25.12	18.20	0.64
PFS _{IDR}	TTPVI	11.30	18.77	<0.01	11.50	7.87	0.96
	RVI	7.43	14.23	0.01	14.23	7.73	0.84
TTP	TTPVI	5.97	15.03	0.03	12.10	7.73	0.27
	RVI	6.40	11.83	0.14	14.23	7.73	0.33
TTP _{LTP}	TTPVI	N/A	N/A	0.63*	N/A	N/A	0.49*
	RVI	N/A	N/A	0.51*	N/A	N/A	0.94*
TTP _{IDR}	TTPVI	9.60	15.67	0.05	12.20	8.00	0.88
	RVI	8.73	15.03	0.21	14.23	8.00	0.52

Notes: N/A non-assessable (*median survival was not reached; however, no significant separation of the curves was achieved). Values are depicted as medians. Bold p-values indicate statistical differences in the Log rank test ($p < 0.05$).

Abbreviations: OS, overall survival; PFS, progression-free survival; TTP, time-to-progression; LTP, local tumor progression; IDR, intrahepatic distant recurrence; TTPVI, two-trait predictor of venous invasion; RVI, radiogenomic venous invasion.

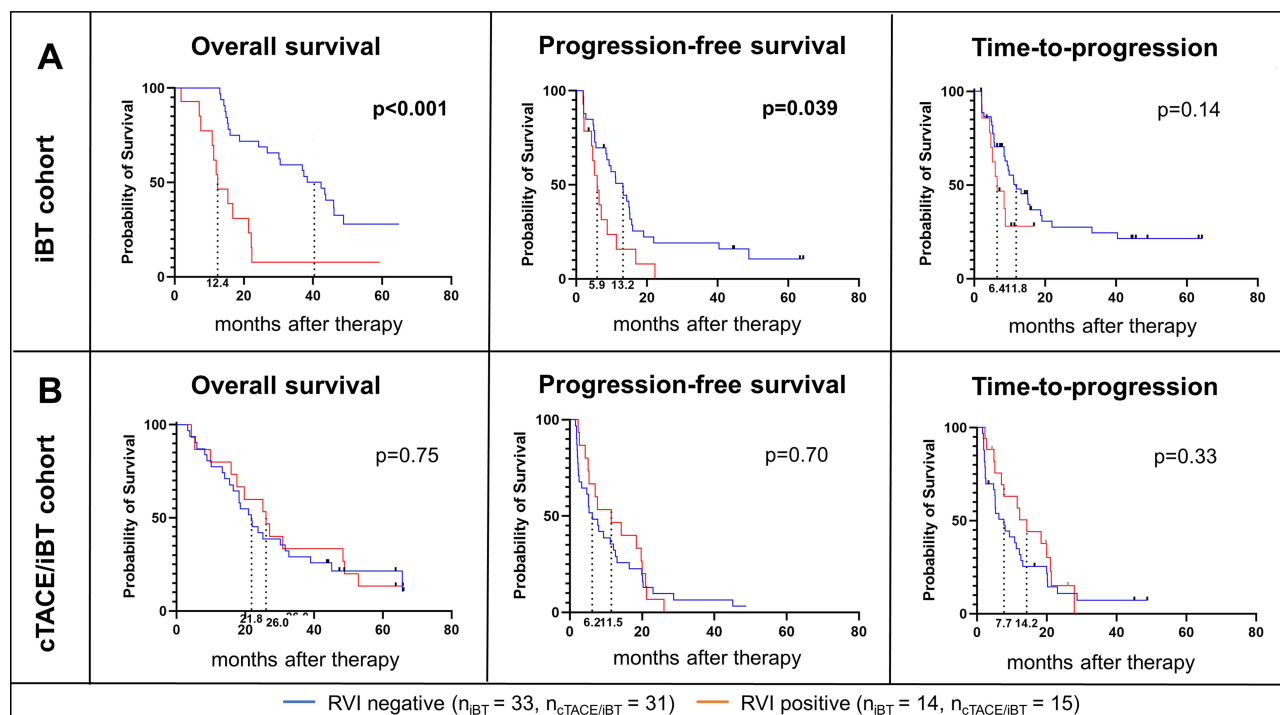


Figure 3 The impact of RVI on patient survival and tumor progression in patients treated with ablation with and without prior embolization. Overall survival (OS), progression-free survival (PFS), and time-to-progression (TTP) are depicted for patients with a positive and negative RVI trait receiving interstitial brachytherapy (iBT, upper row) and iBT with a prior conventional transarterial chemoembolization (cTACE/iBT, lower row). For patients within the iBT group, Kaplan–Meier analysis reveals significantly poorer OS, PFS, and a trend for poorer TTP in patients that had a positive RVI trait. In patients within the cTACE/iBT group, no significant differences in survival outcomes were observed in regards of the RVI trait. Median survival is indicated by dashed lines.

$p = 0.25$), respectively. Similarly, positive RVI and TTPVI traits showed no significant association but revealed trends for poorer OS (positive RVI: 12 months vs negative RVI: median OS not reached, $p = 0.15$; positive TTPVI: 125.8 vs negative TTPVI: 231.7 months, $p = 0.85$) and poorer PFS (RVI 13.1 vs 21.0 months, $p = 0.18$; TTPVI 14.9 vs 67.6 months, $p = 0.24$). Univariate cox-regression analysis confirmed histological MVI as a predictor for PFS ($p = 0.01$), but not for OS. Neither RVI nor TTPVI was confirmed as predictive of OS or PFS, respectively (Figure 4).

Cox Regression Model

In patients treated with iBT, univariate cox-regression analyses confirmed RVI and TTPVI as predictors of OS ($p < 0.01$ and $p = 0.09$), PFS ($p = 0.021$ and $p < 0.01$). TTPVI was also confirmed predictive of TTP ($p = 0.04$) but not RVI ($p = 0.15$). Because no other baseline parameter was found predictive, multivariate analysis was omitted (Table 4). In patients treated with cTACE/iBT, univariate cox-regression analysis revealed age ($p = 0.07$), number of lesions ($p < 0.01$), index lesion diameter ($p < 0.01$), and BCLC stage ($p < 0.01$) as predictors of PFS only (Table 4). In line with the findings from Kaplan–Meier analysis, RVI and TTPVI showed no impact. Multivariate analysis confirmed age ($p = 0.07$) and number of lesions ($p < 0.01$) as significant predictors of PFS.

RVI/TTPVI Correlation with Semantic Imaging Features

For patients in the iBT group, RVI and/or TTPVI were found to significantly correlate with the following semantic imaging features on multiparametric MRI (Table 5): tumoral vessels in arterial phase (RVI: $r = 0.57$, $p < 0.01$ TTPVI: $r = 0.97$, $p < 0.01$) and in portal venous phase (RVI: $r = 0.71$, $p < 0.01$ TTPVI: $r = 0.79$, $p < 0.01$), respectively, peritumoral enhancement (TTPVI: $r = 0.27$, $p = 0.04$), relative tumoral enhancement in portal venous phase (RVI: $r = -0.33$, $p = 0.01$), tumor liver difference in hepatobiliary phase (RVI: $r = 0.28$, $p = 0.03$) and diffusion weighted imaging (RVI: $r = -0.31$, $p = 0.02$), respectively. For patients in the cTACE/iBT group, RVI and/or TTPVI were found to correlate with the following semantic imaging features: tumoral vessels in arterial phase (RVI: $r = 0.32$, $p = 0.03$ TTPVI: $r = 0.30$, $p = 0.03$)

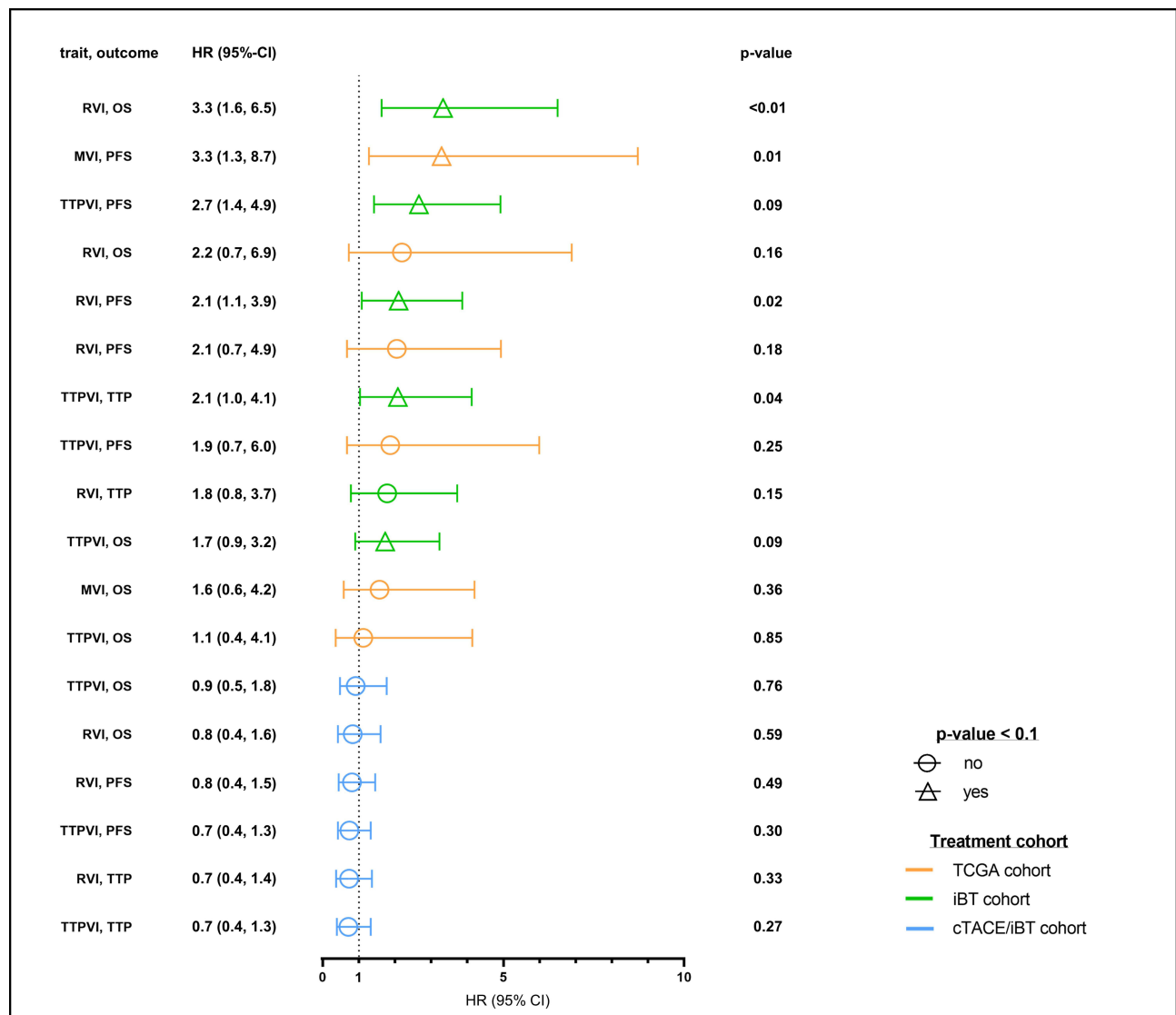


Figure 4 The impact of RVI and TTPVI imaging biomarkers and MVI trait in patients within the internal and external study cohorts. Hazard ratios (HR) and 95% confidence intervals (95%-CI) and p-values were calculated for the impact of RVI, TTPVI in the internal and external study cohorts as well and microvascular invasion (MVI) in the external study cohort and depicted as colored line graphs in the respective colors of the treatment groups: Orange – TCGA cohort, green – interstitial brachytherapy (iBT) cohort, and blue – conventional transarterial chemotherapy with consecutive iBT cohort (cTACE/iBT). Triangles show indicate a significant p-value for the respective Kaplan–Meier analysis ($p < 0.1$).

and in portal venous phase (TTPVI: $r = 0.43$, $p < 0.01$), respectively, irregular arterial phase enhancement pattern (TTPVI: $r = 0.43$, $p < 0.01$), and tumor-liver ratio in diffusion-weighted imaging (TTPVI: $r = -0.35$, $p = 0.02$).

Discussion

This study was designed to establish the decision-tree models RVI and TTPVI indicative of histological MVI on multiparametric contrast-enhanced liver MRI and investigate their prognostic value for the clinical outcome in patients with unresectable HCC undergoing LRT. Following validation on the external TCGA-LIHC database, both RVI and TTPVI were found to be associated with poorer OS, PFS, and TTP in patients who received ablation via iBT alone. However, in patients treated with additional cTACE prior to iBT, neither RVI nor TTPVI was associated with patient survival. These findings suggest that patients with positive RVI or TTPVI on baseline MRI may benefit from combined embolization prior to ablation to address probable MVI that remains relatively occult on standard liver MRI readings.

Table 4 The Confounding Effects of Clinical Parameters on the Survival Outcomes

iBT Cohort									
	Overall Survival			Progression-Free Survival			Time-to-Progression		
	95% CI	HR	p-value	95% CI	HR	p-value	95% CI	HR	p-value
Age	0.95–1.02	0.96	0.40	0.97–1.03	1.00	0.92	0.96–1.03	0.99	0.65
Gender	0.40–1.67	0.78	0.49	0.56–1.27	1.06	0.86	0.48–2.15	0.96	0.92
Index tumor diameter	0.98–1.04	1.01	0.44	0.97–1.03	1.00	0.93	0.95–1.02	0.99	0.44
Number of lesions	0.68–1.21	0.94	0.66	0.90–1.65	1.25	0.15	0.91–1.77	1.31	0.11
BCLC stage	0.51–2.77	1.31	0.53	0.63–2.89	1.48	0.31	0.47–2.86	1.32	0.54
RVI	1.63–6.50	3.33	<0.01	1.08–3.86	2.10	0.02	0.78–3.72	1.78	0.15
TTPVI	0.90–3.23	1.73	0.09	1.42–4.92	2.66	<0.01	1.03–4.12	2.08	0.04
0.01									
cTACE/iBT Cohort									
	Overall Survival			Progression-Free Survival			Time-to-Progression		
	95% CI	HR	p-value	95% CI	HR	p-value	95% CI	HR	p-value
Age	0.93–1.00	0.97	0.07	0.97–1.04	1.00	0.93	0.96–1.03	1.00	0.89
Gender	0.40–1.98	0.84	0.66	0.55–2.23	1.07	0.86	0.44–1.84	0.86	0.68
Index tumor diameter	1.01–1.03	1.02	<0.01	0.98–1.01	1.00	0.60	0.98–1.01	1.00	0.60
Number of lesions	1.27–3.62	2.19	<0.01	0.68–1.64	1.09	0.70	0.35–1.16	0.68	0.20
BCLC stage	1.15–2.58	1.73	<0.01	0.80–1.73	1.19	0.37	0.74–1.68	1.13	0.56
RVI	0.42–1.60	0.83	0.59	0.44–1.45	0.81	0.49	0.37–1.36	0.73	0.33
TTPVI	0.48–1.77	0.91	0.76	0.42–1.33	0.74	0.30	0.39–1.33	0.71	0.27
TCGA-LIHC Cohort									
	Overall Survival			Progression-Free Survival					
	95% CI	HR	p-value	95% CI	HR	p-value			
MVI	0.58–4.20	1.57	0.36	1.28–8.72	3.29	0.01			
RVI	0.72–6.89	2.19	0.16	0.67–5.93	2.05	0.18			
TTPVI	0.36–4.14	1.12	0.85	0.67–5.99	1.87	0.25			

Note: Bold print p-values indicate statistical differences in the regression analyses ($p < 0.1$).

Abbreviations: iBT, interstitial brachytherapy; cTACE, conventional transarterial chemoembolization; TCGA-LIHC, The Cancer Genome Atlas – Liver Hepatocellular Carcinoma (public external database); MVI, microvascular invasion; RVI, Radiogenomic Venous Invasion; TTPVI, Two Trait Predictor of Venous Invasion; HR, hazard ratio; 95% CI, 95% confidence interval.

Both RVI and TTPVI represent vascularity grading systems that support the probability of varying micro vascularization by considering ancillary findings on contrast-enhanced imaging. In this study, RVI and TTPVI were found to correlate with a variety of semantic features, which supports the hypothesis that MVI is a rather complex tumor component that cannot be reflected by a single ancillary imaging feature, but rather a systematic review of many vascular imaging features. Although some of those semantic features may be routinely assessed and possibly described in liver MRI readings, their collective value for the prognosis of HCC patients remains underappreciated. Additionally, imaging biomarker traits may be underrepresented in current HCC guidelines, e.g. the Barcelona Clinic and Liver-Cancer

Table 5 Correlation of Semantic Imaging Features with Radiogenomic Venous Invasion (RVI) and Two-Trait Predictor of Venous Invasion (TTPVI)

Semantic Imaging Feature	Imaging Biomarker	iBT Cohort		cTACE/iBT Cohort	
		Pearson's r	p-value	Pearson's r	p-value
Vessel in lesion (art.)	TTPVI	0.97	<0.01	0.30	0.03
	RVI	0.57	<0.01	0.32	0.03
Vessel in lesion (pv.)	TTPVI	0.79	<0.01	0.43	<0.01
	RVI	0.71	<0.01	0.04	0.77
Enhancement pattern (art.)	TTPVI	-0.22	0.10	0.43	<0.01
	RVI	-0.23	0.08	0.04	0.77
Perilesional enhancement (art.)	TTPVI	0.27	0.04	0.09	0.49
	RVI	0.16	0.23	-0.02	0.90
Perilesional hypointensity (HBP)	TTPVI	0.24	0.08	0.23	0.11
	RVI	0.11	0.41	0.07	0.62
Tumor margin (ven.)	TTPVI	-0.16	0.23	-0.03	0.84
	RVI	-0.17	0.20	0.17	0.26
Tumor capsule (ven.)	TTPVI	0.13	0.32	-0.10	0.50
	RVI	0.03	0.82	-0.01	0.93
Relative tumoral enhancement (art.)	TTPVI	0.01	0.92	0.07	0.65
	RVI	-0.10	0.12	-0.23	0.12
Relative tumoral enhancement (pv.)	TTPVI	-0.16	0.23	0.07	0.61
	RVI	-0.33	0.01	-0.04	0.76
Tumor liver ratio (HBP)	TTPVI	0.01	0.98	-0.04	0.78
	RVI	0.28	0.03	-0.01	0.96
Tumor liver ratio (DWI)	TTPVI	-0.01	0.98	-0.35	0.02
	RVI	-0.31	0.02	0.07	0.67
Tumor liver ratio (ADC)	TTPVI	0.07	0.63	-0.24	0.10
	RVI	-0.04	0.74	0.11	0.44

Note: Bold p-values (and respective Pearson's r) indicate statistical significance ($p < 0.05$).

Abbreviations: TTPVI, two-trait predictor of venous invasion; RVI, radiogenomic venous invasion; Art, arterial phase; pv, portal venous phase; ven, venous phase; HBP, hepatobiliary phase of T1-weighted images; DWI, diffusion weighted imaging; ADC, apparent diffusion coefficient maps; iBT, interstitial brachytherapy; cTACE, conventional transarterial chemoembolization.

(BCLC) classification considers only tumor multiplicity, size, and macrovascular invasion for disease staging and treatment recommendation.²⁷ Meanwhile, the Clinical Practice Guidelines of the European Association for the Study of the Liver (EASL) underscore the role of CECT and multiparametric MRI diagnosis and staging of HCC and consider major imaging features such as hyperenhancement, washout, and capsule enhancement to reflect general vascular derangement during hepatocarcinogenesis.^{28,29}

However, in clinical routine, decisions on LRT allocation are frequently made at the discretion of the interventional radiologist for lack of more specific guidelines, taking into account additional imaging features such as patterns of

arterial hyperenhancement and the presence of large tumor-feeding arteries.^{30,31} Additional, potentially useful imaging features have been reported to be associated with the prognosis of HCC.^{32–34} However, they are usually based on visual estimations, and are not assessed systematically, posing a substantial barrier for routine clinical use.

Therefore, novel research is focused on linking radiological imaging features with gene profile analysis to derive standardized radiological imaging biomarkers that reflect the individual biological tumor phenotype and enable a more precise prediction of early recurrence and tumor progression.^{14,15} Although MVI represents a complex biological tumor component, RVI and TTPVI are promising candidates to non-invasively capture the presence of histological MVI in HCC.³⁵ Both have been repeatedly validated by rad-path analyses in previous studies to facilitate their clinical application without the need for additional tissue biopsies.^{16,17} Since these imaging biomarkers are derived from genomic analyses, previous studies indicated that they could represent a more fundamental phenotype of aggressive disease than MVI itself.^{12,13} Specifically, Banerjee et al showed that RVI was predictive of OS and recurrence-free survival, whereas histological MVI was not.¹⁴ This observation could explain our study's finding of the merely acceptable to low correlation with histological MVI in the TCGA-LIHC cohort. However, RVI detected MVI with a relatively high specificity (88.9%) but rather low sensitivity (69.2%), while TTPVI showed a relatively high sensitivity (84.6%) but only low specificity (50.0%).

However, the consistency in detecting MVI based on histology may also lack due to tissue procurement and intratumoral heterogeneity causing sampling errors.³⁶ Moreover, substantial evidence exists, supporting not only the tumoral core but also the peritumoral zone to play a key role in angiogenesis and metastatic disease. In this regard, peripheral vessel encapsulating tumor clusters (VECTS) has recently been described as distinct vascular patterns seen in HCC histology that can serve as a risk factor for recurrent disease, and thus, may be adequately treated with embolotherapies.³⁷

Regarding the sub-analyses of local progression patterns, no significant correlation with TTP_{LTP} was found in both our treatment groups, emphasizing LRT to achieve very good local tumor control independent of RVI or TTPVI status. However, regarding the distant intrahepatic progression pattern, both imaging biomarkers were associated with shorter PFS_{IDR} and TTP_{IDR} in patients treated with iBT. This may support the hypothesis that the imaging biomarkers of RVI and TTPVI also reflect a more severe live disease but not only tumor phenotype in patients with HCC, which in return is more likely to contribute to new intrahepatic distant lesions.³⁸

The results further suggest ablative LRT regimens to be insufficient treatments for the subgroup with high likelihood of a more aggressive, vascularization-dependent HCC phenotype. Similarly, Imai et al reported on patients with MVI-positive HCC undergoing radiofrequency ablation to have worse OS supporting the hypothesis of RVI and TTPVI to reflect a more aggressive HCC subtype that relies on extensive blood supply.³⁹ In turn, besides many other yet unexplored variables, such patients may potentially benefit from additional embolization therapy as previous studies investigated the role of cTACE to effectively address histological MVI in HCC patients following surgical regimens,⁴⁰ showing that preoperative cTACE may possibly affect disease-free and OS rates in HCC patients following liver resection.⁴¹ In our institution, cTACE prior to iBT is frequently performed, if tumors show arterial hyperenhancement or distinct tumor feeding arteries or exceed 5 cm in diameter. Additionally, cTACE can be performed in smaller lesions to deposit Lipiodol in the tumor and guide the puncture and ablation under CT-guidance.

Overall, our findings in the presence of RVI are in good concordance with the original reports from Banerjee et al, in which 26.1% of the patients with HCC undergoing surgical resection were detected RVI positive.¹⁴ As for TTPVI, in the original study by Renzulli et al, 57.8% of the HCC patients undergoing hepatic resection were detected with TTPVI positive.¹⁵ Li et al detected TTPVI in 44.3%,¹⁶ whereas Zhang et al detected in 83%⁴² of their study patients, suggesting TTPVI assessment to be more variable than RVI. However, in all studies, TTPVI was found to be highly predictive of MVI, showing a strong correlation with poor survival, which is in line with our findings for the TCGA-LIHC and iBT cohort.

This study has some limitations. Due to the retrospective study design, demographics of the internal cohorts showed some differences but were overall comparable. Specifically, lesion size and BCLC stage were more advanced in patients following cTACE/iBT since the decision-making process for a suitable LRT regimen depends on these features. Additionally, tumor size and stage may represent potential bias for treatment response and patient survival.⁴³ However, cox-regression revealed no predictors in the entirety of the study cohort (data not shown) and no difference in survival curves was found. Although iBT is approved for the treatment of early-stage HCC according to ESMO

guidelines,⁴⁴ it is performed less frequently than thermal ablation. Given the different mechanisms of action of both ablative techniques, the reproducibility of the findings in the context of thermal ablation needs to be further investigated. This study supports the feasibility of assessing imaging biomarkers in contrast-enhanced MRI using gadoxetic-acid-disodium (Primovist) as a contrast agent; however, robustness and reproducibility need further investigation. Additional MRI sequences such as diffusion-weighted imaging, hepatobiliary phases or other semantic imaging features that have been previously reported to be associated with HCC subtypes have only been considered for the image-based diagnosis of HCC but were not considered in the decision-tree models. The imaging biomarkers of RVI and TTPVI have been independently assessed by two readers, who finally found a common consent on the status of these parameters. However, no interclass correlation coefficients have been calculated since it has already been reported elsewhere.¹⁷ Therefore, an external dataset validation was used; however, it provides data from the early 2000s and therefore lacks newest techniques in histological confirmation and biomedical imaging.

Conclusion

In conclusion, this study established and validated RVI and TTPVI as imaging biomarkers indicative of MVI on multiparametric liver MRI to estimate survival in patients with HCC undergoing LRT. Both RVI and TTPVI were associated with poorer survival and tumor recurrence in patients following ablation via iBT alone but showed no association with the outcome after combined cTACE and iBT. Thus, such non-invasive tools may be key for improved patient stratification and personalized treatment planning by identifying HCC patients with occult vascular invasion on baseline MRI, who would potentially benefit from additional embolotherapy prior to ablation rather than ablation alone. Moreover, this study emphasizes the unmet need of considering HCC tumoral heterogeneity as detected in pre-procedural imaging to be incorporated into the current management and treatment algorithms in the future.

Abbreviations

iBT, interstitial brachytherapy; cTACE, conventional transarterial chemoembolization; ALT, alanine aminotransferase; AST, aspartate aminotransferase; γ -GT, gamma-glutamyl transferase; AP, alkaline phosphatase; CR, complete response; PR, partial response; SD, stable disease; PD, progressive disease; OS, overall survival; PFS, progression-free survival; TTP, time-to-progression; LTP, local tumor progression; IDR, intrahepatic distant recurrence, TCGA-LIHC, The Cancer Genome Atlas, Liver Hepatocellular Carcinoma (public external database); art., arterial phase; pv., portal venous phase; ven., venous phase; HBP, hepatobiliary phase of T1-weighted images; DWI, diffusion weighted imaging; ADC, apparent diffusion coefficient maps.

Data Sharing Statement

Additional data are available to readers upon reasonable request to the corresponding author.

Ethical Approval

Institutional Review Board approval by the Charité – University Medicine Berlin's human research committee was obtained.

Statistics and Biometry

No complex statistical methods were necessary for this paper.

Informed Consent

Informed consent was waived due to the retrospective study design.

Study Subjects or Cohorts Overlap

No study subjects or cohorts have been previously reported.

Acknowledgments

Parts of this work have been presented at the SIO Annual Meeting 2022, ECR Overture 2022, CIRSE 2022, and RSNA 2022, respectively. The authors like to thank Prof. Dr. Bernd Hamm for his guidance and supervision in- and outside the submitted work.

Author Contributions

All authors made a significant contribution to the work reported, whether that is in the conception, study design, execution, acquisition of data, analysis and interpretation, or in all these areas; took part in drafting, revising or critically reviewing the article; gave final approval of the version to be published; have agreed on the journal to which the article has been submitted; and agree to be accountable for all aspects of the work.

Disclosure

The authors state that this work has not received any funding. The authors of this manuscript declare no relationships with any companies, whose products or services may be related to the subject matter of the article. Outside the submitted work, RS received a stipend from Berliner Krebsgesellschaft e.V.. CAH and LJS are currently fellows of the BIH Charité (Junior Digital) Clinician Scientist Program funded by the Charité-Universitätsmedizin Berlin and the Berlin Institute of Health. HX and YH are fellows of the Chinese Scholarship Council. LJS receives research grants from the Berliner Krebsgesellschaft e.V., the Collaborative Research Center (CRC) 1340 “Matrix in Vision” funded by the Deutsche Forschungsgemeinschaft (DFG), the DFG research unit 5628 “Multiscale MRE: in vivo physics of cancer”, and Guerbet, and honoraria and travel support from Guerbet. Outside the submitted work, BG reports honoraria and travel support in the last 10 years from Parexel/CALYX, C.R. BARD/BD, SIRTex Medical, St. Jude Medical, COOK, AngioDynamics, Pharmcept, Guerbet, Ewimed, Siemens, VARIAN, Terumo, Roche, Merck, 3M, Beacon Bioscience/ICON, IPSEN, Bayer, Pfizer, Eisai, MSD, and INARI; grants from INARI, Siemens, SIRTEx, BARD/BD. The authors report no other conflicts of interest in this work.

References

1. Sung H, Ferlay J, Siegel RL, et al. Global Cancer Statistics 2020: GLOBOCAN Estimates of Incidence and Mortality Worldwide for 36 Cancers in 185 Countries. *CA Cancer J Clin*. 2021;71(3):209–249.
2. Bruix J, Sherman M. Management of hepatocellular carcinoma. *Hepatology*. 2005;42(5):1208–1236.
3. Yau T, Tang VY, Yao TJ, Fan ST, Lo CM, Poon RT. Development of Hong Kong Liver Cancer staging system with treatment stratification for patients with hepatocellular carcinoma. *Gastroenterology*. 2014;146(7):1691–1700.e1693.
4. Schnapauff D, Tegel BR, Powerski MJ, Colletini F, Hamm B, Gebauer B. Interstitial Brachytherapy in Combination With Previous Transarterial Embolization in Patients With Unresectable Hepatocellular Carcinoma. *Anticancer Res*. 2019;39(3):1329–1336.
5. Colletini F, Singh A, Schnapauff D, et al. Computed-tomography-guided high-dose-rate brachytherapy (CT-HDRBT) ablation of metastases adjacent to the liver hilum. *Eur J Radiol*. 2013;82(10):e509–514.
6. Schnapauff D, Colletini F, Hartwig K, et al. CT-guided brachytherapy as salvage therapy for intrahepatic recurrence of HCC after surgical resection. *Anticancer Res*. 2015;35(1):319–323.
7. Colletini F, Schnapauff D, Poellinger A, et al. Hepatocellular carcinoma: computed-tomography-guided high-dose-rate brachytherapy (CT-HDRBT) ablation of large (5–7 cm) and very large (>7 cm) tumours. *Eur Radiol*. 2012;22(5):1101–1109.
8. Zuo TY, Liu FY, Wang MQ, Chen XX. Transcatheter Arterial Chemoembolization Combined with Simultaneous Computed Tomography-guided Radiofrequency Ablation for Large Hepatocellular Carcinomas. *Chin Med J*. 2017;130(22):2666–2673.
9. Jeng KS, Chang CF, Jeng WJ, Sheen IS, Jeng CJ. Heterogeneity of hepatocellular carcinoma contributes to cancer progression. *Crit Rev Oncol Hematol*. 2015;94(3):337–347.
10. Zheng Z, Guan R, Jianxi W, et al. Microvascular Invasion in Hepatocellular Carcinoma: a Review of Its Definition, Clinical Significance, and Comprehensive Management. *J Oncol*. 2022;2022:9567041.
11. Lim KC, Chow PK, Allen JC, et al. Microvascular invasion is a better predictor of tumor recurrence and overall survival following surgical resection for hepatocellular carcinoma compared to the Milan criteria. *Ann Surg*. 2011;254(1):108–113.
12. Chen X, Cheung ST, So S, et al. Gene expression patterns in human liver cancers. *Mol Biol Cell*. 2002;13(6):1929–1939.
13. Segal E, Sirlin CB, Ooi C, et al. Decoding global gene expression programs in liver cancer by noninvasive imaging. *Nat Biotechnol*. 2007;25(6):675–680.
14. Banerjee S, Wang DS, Kim HJ, et al. A computed tomography radiogenomic biomarker predicts microvascular invasion and clinical outcomes in hepatocellular carcinoma. *Hepatology*. 2015;62(3):792–800.
15. Renzulli M, Brocchi S, Cucchetti A, et al. Can Current Preoperative Imaging Be Used to Detect Microvascular Invasion of Hepatocellular Carcinoma? *Radiology*. 2016;279(2):432–442.

16. Li X, Zhang X, Li Z, et al. Two-Trait Predictor of Venous Invasion on Contrast-Enhanced CT as a Preoperative Predictor of Outcomes for Early-Stage Hepatocellular Carcinoma After Hepatectomy. *Front Oncol.* 2021;11:688087.
17. Bakr S, Gevaert O, Patel B, et al. Interreader Variability in Semantic Annotation of Microvascular Invasion in Hepatocellular Carcinoma on Contrast-enhanced Triphasic CT Images. *Radiol Imaging Cancer.* 2020;2(3):e190062.
18. American College of Radiology Committee on LI-RADS®. LI-RADS Assessment Categories 2018. Available from: <https://www.acr.org/-/media/ACR/Files/RADS/LI-RADS/Translations/LI-RADS-2018-CT-MRI-Core-German.pdf>. Accessed June 5, 2024.
19. National Cancer Institute. The Cancer Genome Atlas - Liver Hepatocellular Carcinoma (TCGA-LIHC) database. Available from: <https://portal.gdc.cancer.gov/projects/TCGA-LIHC>. Accessed June 5, 2024.
20. Ricke J, Wust P, Stohlmann A, et al. CT-guided interstitial brachytherapy of liver malignancies alone or in combination with thermal ablation: Phase I-II results of a novel technique. *Int J Radiat Oncol Biol Phys.* 2004;58(5):1496–1505.
21. Bretschneider T, Ricke J, Gebauer B, Streitparth F. Image-guided high-dose-rate brachytherapy of malignancies in various inner organs - technique, indications, and perspectives. *J Contemp Brachytherapy.* 2016;8(3):251–261.
22. Mohnike K, Wieners G, Schwartz F, et al. Computed tomography-guided high-dose-rate brachytherapy in hepatocellular carcinoma: safety, efficacy, and effect on survival. *Int J Radiat Oncol Biol Phys.* 2010;78(1):172–179.
23. Lencioni R, Llovet JM. Modified RECIST (mRECIST) assessment for hepatocellular carcinoma. *Semin Liver Dis.* 2010;30(1):52–60.
24. Mariotto AB, Noone AM, Howlader N, et al. Cancer survival: an overview of measures, uses, and interpretation. *J Natl Cancer Inst Monogr.* 2014;2014(49):145–186.
25. Ahmed M, Solbiati L, Brace CL, et al. Image-guided tumor ablation: standardization of terminology and reporting criteria—a 10-year update. *Radiology.* 2014;273(1):241–260.
26. Xu H, Schmidt R, Hamm CA, et al. Comparison of intrahepatic progression patterns of hepatocellular carcinoma and colorectal liver metastases following CT-guided high dose-rate brachytherapy. *Ther Adv Med Oncol.* 2021;13:17588359211042304.
27. Llovet JM, Brú C, Bruix J. Prognosis of hepatocellular carcinoma: the BCLC staging classification. *Semin Liver Dis.* 1999;19(3):329–338.
28. Galle PR. EASL Clinical Practice Guidelines: management of hepatocellular carcinoma. *J Hepatol.* 2018;69(1):182–236.
29. Cunha GM, Sirlin CB, Fowler KJ. Imaging diagnosis of hepatocellular carcinoma: LI-RADS. *Chin Clin Oncol.* 2021;10(1):3.
30. Lencioni R, Crocetti L. Local-regional treatment of hepatocellular carcinoma. *Radiology.* 2012;262(1):43–58.
31. Jezzi R, Pompili M, Posa A, Coppola G, Gasbarrini A, Bonomo L. Combined locoregional treatment of patients with hepatocellular carcinoma: state of the art. *World J Gastroenterol.* 2016;22(6):1935–1942.
32. An C, Kim MJ. Imaging features related with prognosis of hepatocellular carcinoma. *Abdom Radiol.* 2019;44(2):509–516.
33. Khatri G, Merrick L, Miller FH. MR imaging of hepatocellular carcinoma. *Magn Reson Imaging Clin N Am.* 2010;18(3):421–450, x.
34. Cho E-S, Choi J-Y. MRI Features of Hepatocellular Carcinoma Related to Biologic Behavior. *Korean J Radiol.* 2015;16(3):449.
35. Rodríguez-Perálvarez M, Luong TV, Andreana L, Meyer T, Dhillon AP, Burroughs AK. A systematic review of microvascular invasion in hepatocellular carcinoma: diagnostic and prognostic variability. *Ann Surg Oncol.* 2013;20(1):325–339.
36. Pawlik TM, Gleisner AL, Anders RA, Assumpcao L, Maley W, Choti MA. Preoperative assessment of hepatocellular carcinoma tumor grade using needle biopsy: implications for transplant eligibility. *Ann Surg.* 2007;245(3):435–442.
37. Wang JH, Li XS, Tang HS, et al. Vessels that encapsulate tumor clusters (VETC) pattern predicts the efficacy of adjuvant TACE in hepatocellular carcinoma. *J Cancer Res Clin Oncol.* 2023;149(8):4163–4172.
38. Tang H, Bai HX, Su C, Lee AM, Yang L. The effect of cirrhosis on radiogenomic biomarker's ability to predict microvascular invasion and outcome in hepatocellular carcinoma. *Hepatology.* 2016;64(2):691–692.
39. Imai K, Yamashita YI, Yusa T, et al. Microvascular Invasion in Small-sized Hepatocellular Carcinoma: significance for Outcomes Following Hepatectomy and Radiofrequency Ablation. *Anticancer Res.* 2018;38(2):1053–1060.
40. Chen ZH, Zhang XP, Zhou TF, et al. Adjuvant transarterial chemoembolization improves survival outcomes in hepatocellular carcinoma with microvascular invasion: a systematic review and meta-analysis. *Eur J Surg Oncol.* 2019;45(11):2188–2196.
41. Yang Y, Lin K, Liu L, et al. Impact of preoperative TACE on incidences of microvascular invasion and long-term post-hepatectomy survival in hepatocellular carcinoma patients: a propensity score matching analysis. *Cancer Med.* 2021;10(6):2100–2111.
42. Zhang T, Pandey G, Xu L, et al. The Value of TTPVI in Prediction of Microvascular Invasion in Hepatocellular Carcinoma. *Cancer Manag Res.* 2020;12:4097–4105.
43. Xu W, Wang Y, Yang Z, Li J, Li R, Liu F. New Insights Into a Classification-Based Microvascular Invasion Prediction Model in Hepatocellular Carcinoma: a Multicenter Study. *Front Oncol.* 2022;12:796311.
44. Vogel A, Cervantes A, Chau I, et al. Hepatocellular carcinoma: ESMO Clinical Practice Guidelines for diagnosis, treatment and follow-up. *Ann Oncol.* 2018;29(Suppl 4):548.